International Journal of Remote Sensing
Publication details, including instructions for authors and subscription information:
http://www.tandfonline.com/loi/tres20

An operational method to estimate evapotranspiration using MODIS data during winter wheat growing season

Yonghong Yi [a b] & Dawen Yang [a]

[a] State Key Laboratory of Hydro-Science and Engineering, Department of Hydraulic Engineering, Tsinghua University, Beijing, 100084, PR, China

[b] The Numerical Terradynamic Simulation Group, University of Montana, Missoula, MT, 59812, USA

Available online: 6 July 2011

To cite this article: Yonghong Yi & Dawen Yang (2011): An operational method to estimate evapotranspiration using MODIS data during winter wheat growing season, International Journal of Remote Sensing, DOI:10.1080/01431161.2010.492252

To link to this article: http://dx.doi.org/10.1080/01431161.2010.492252

International Journal of Remote Sensing
iFirst, 2011, 1–18

An operational method to estimate evapotranspiration using MODIS data during winter wheat growing season

YONGHONG YI†‡ and DAWEN YANG*†

†State Key Laboratory of Hydro-Science and Engineering, Department of Hydraulic Engineering, Tsinghua University, Beijing, 100084, PR China.
‡The Numerical Terradynamic Simulation Group, University of Montana, Missoula, MT, 59812, USA

(*Received 1 July 2009; in final form 28 September 2009*)

The Penman–Monteith (P-M) model has been widely used to estimate actual evapotranspiration (ET). However, its application is mainly constrained to within field scales because the surface resistance under water stress at large scales is difficult to define. The Normalized Difference Water Index (NDWI) derived from Moderate Resolution Imaging Spectroradiometer (MODIS) data was shown to be sensitive to the crop water content and water deficit, and used to estimate the surface resistance in the P-M model. The modelled latent heat fluxes matched well with the eddy correlation observations, and the spatial distributions also showed a similar pattern as the results from the one-layer model in an irrigated area at the downstream of Yellow River. To reduce the influence of cloud and other atmospheric disturbances, the daily surface resistance was retrieved from 8-day temporal composite MODIS NDWI. The modelled daily ET showed consistent temporal changes with the observations during the wheat growing season. This method showed advantages over the other remote sensing models, for example, the one-layer model, which required daily radiative temperature inputs and cannot be implemented under cloudy conditions.

1. Introduction

Water shortage and uneven distribution of precipitation in time and space are major limiting factors for the economic development and agricultural production in the Northern China Plain. Winter wheat is the major crop in this area from winter to spring, and its growth is greatly influenced by the rainfall distribution during this period. The decreasing precipitation and increasing air temperature in this area due to climate change mean that more crop irrigation is necessary, especially during the winter wheat season (Yang *et al.* 2004, Cracknell and Varotsos 2007), and the water conflict between irrigation and industrial use is becoming severe in the Yellow River basin. To better manage the limited water resources, accurate assessment of crop water consumption is required. Field sampling has been extensively used to measure crop water consumption or actual evapotranspiration (ET) and estimate water stress by measuring soil moisture from a scale of several metres up to several hundreds of metres. However, it is difficult to make regional estimates from field observations due to large heterogeneities in land cover and plantation (Maayar and Chen 2006). Remote sensing data have obvious advantages over field observations and are widely used for regional

*Corresponding author. Email: yangdw@tsinghua.edu.cn

International Journal of Remote Sensing
ISSN 0143-1161 print/ISSN 1366-5901 online
http://www.tandf.co.uk/journals
DOI: 10.1080/01431161.2010.492252

water cycle studies since they can provide measurements of land surface status over large areas (Jupp *et al.* 1998, Jiang and Islam 1999, Nishida *et al.* 2003, Su *et al.* 2003).

Derivation of ET estimates from remote sensing data is based on assessing the surface energy balance by observing surface properties such as albedo, vegetation cover, leaf area index (LAI) and surface temperature (Bastiaanssen *et al.* 1998, Jupp *et al.* 1998). The available net radiation energy is partitioned into soil heat and atmospheric convective fluxes including sensible heat and latent heat. The main differences between remote sensing models lie in the treatment of the observed surface and the parameterization of the radiant and convective fluxes (Courault *et al.* 2005). The one-layer approach considers the land surface as a single component, while the two-layer or multilayer approaches discriminate the soil and vegetation components, with different characterization of canopy structure. The one-layer model is easy to run, but the aerodynamic temperature defined in the model is generally different from the surface temperature derived from remote sensing especially under sparse vegetation conditions (Chehbouni *et al.* 1996, Su *et al.* 2001). The two-layer model incorporates the difference between the two temperatures. However, it is difficult to solve the model without knowing the soil and vegetation component temperatures when only one observation of radiometric temperature is available (Norman *et al.* 1995, Kustas and Norman 1999, French *et al.* 2005). Therefore, empirical assumptions have to be introduced to solve the model due to the absence of satellite multi-angle thermal-infrared sensors. Two methods are usually used: one builds the empirical relationship between radiometric temperature and the component temperatures (or aerodynamic temperature) (Chehbouni *et al.* 2001); the other method reduces the two-layer model into a modified single-layer model by providing an extra condition (Norman *et al.* 1995, Jupp *et al.* 1998, Kustas and Norman 1999, French *et al.* 2005). As an example of the second method, the Priestley–Taylor (P-T) equation is usually applied to initialize the canopy transpiration, assuming the vegetation has suffered no water stress (e.g. Norman *et al.* 1995).

All the above models are sensitive to the uncertainty of the surface temperature retrieval, which relies on remote sensing techniques and shows great uncertainty (Wan *et al.* 2002). The surface temperature is very sensitive to atmospheric movement; methods for describing the corresponding fluctuation in surface temperature have been widely investigated but not on the satellite observed temperature (Katul *et al.* 1998, Varotsos 2005, Varotsos *et al.* 2007). The Penman–Monteith (P-M) model eliminates the need for surface temperature and has been widely used for evaporation modelling, but mostly at field scales (Courault *et al.* 2005). This is because the surface resistance under unsaturated surfaces at large scales is usually difficult to estimate without intensive sampling of soil moisture and crop growth parameters (Moran *et al.* 1994, Cleugh *et al.* 2007, Mu *et al.* 2007). Therefore, the main objective of this article is to retrieve surface resistance from remote sensing data and extend the application of P-M model at a regional scale.

The Moderate Resolution Imaging Spectroradiometer (MODIS) onboard the Terra and Aqua satellites provides observations twice a day on a near-daily basis (every other day at the equator) at moderate spatial resolutions from 250 to 1000 m, which makes it appealing for regional water and energy cycles monitoring (Kustas *et al.* 2003, Cleugh *et al.* 2007, Mu *et al.* 2007). Although sensors with higher spatial resolution, for Example, Landsat Thematic Mapper (TM) or Enhanced Thematic Mapper (ETM) and Advanced Spaceborne Thermal Emission and Reflection Radiometer (ASTER), are more desirable, these sensors have much lower temporal resolution, and cloud contamination limits their application to monitoring of crop water use on

a regular basis, as is needed for irrigation management. Moreover, the publication of MODIS land surface products facilitates their application to ecology and hydrology modelling without needing to make atmospheric and radiometric correction.

The objective of this article is to develop an operational method based on the P-M model and MODIS data to estimate daily crop water consumption in an irrigated area located at the downstream part of the Yellow River, to provide support for optimized irrigation management. A water index derived from MODIS data was used to estimate the surface resistance in P-M model, and the results were validated using field flux observations and compared with the popular one-layer model.

2. Methodology

2.1 *Study area and field experiments*

Field experiments have been carried out around an eddy flux tower (116° 3′ 15.3″ E, 36° 38′ 55.5″ N, 30 m elevation) in the Weishan Irrigation Zone (WIZ) (115° 24′–116° 30′ E, 36° 12′–37° 00′ N) since April 2005. The WIZ and the location and surroundings of the field experiment site are shown in figure 1. Within a radius of several kilometres around the flux tower the croplands area is almost homogeneously covered by the same crop. This region is part of the Northern China Plain and also the largest irrigation zone in the downstream area of the Yellow River with a total area of 3600 km^2. Three major channels provide irrigation for most of the area, with water taken from the Yellow River in the south-eastern part. The rotation of winter wheat

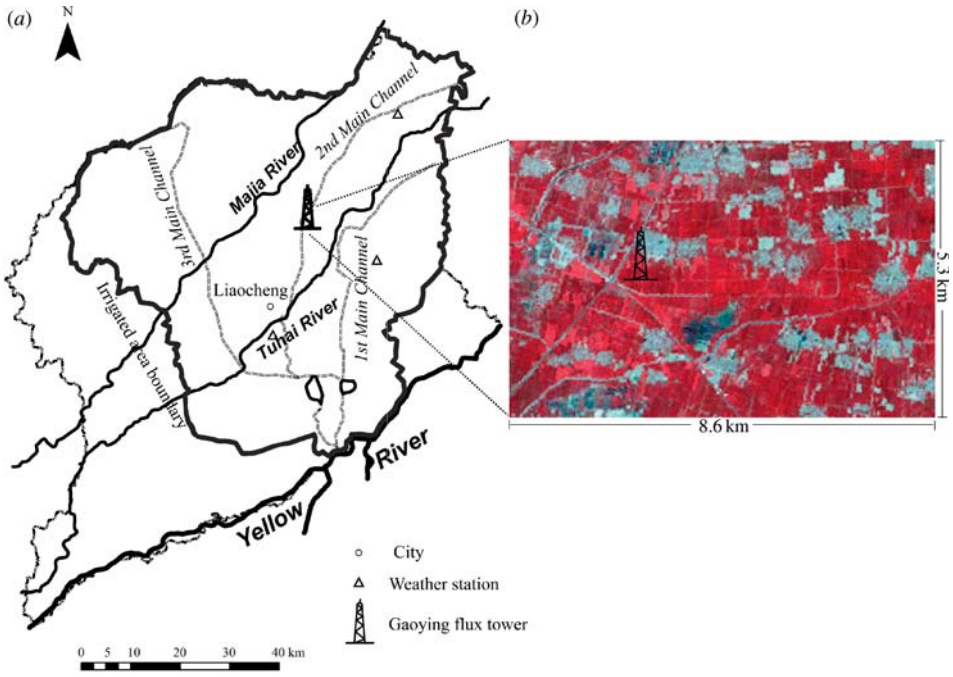

Figure 1. The study area and the field site. (*a*) Weishan irrigation zone along the downstream part of the Yellow River and the locations of the flux tower and three weather stations. (*b*) The location of the flux tower for validation and its surroundings. The background is a false-colour composite Landsat ETM image on 16 May 2000 (30 m, bands 4, 3, 2).

and summer corn is the local primary agricultural practice with crop plantation occupying over 80% of the total area. The winter wheat season occurs between October and June. Multi-year averaged precipitation in this zone is around 571 mm, of which over 60% falls in the summer and less than 20% falls in the spring. Two or three applications of irrigation are usually made during the fast-growing period of wheat in the dry season, from March to May.

The flux tower was equipped with a net radiometer, soil heat flux plates and an eddy covariance system. The energy balance closure was around 80% from the spring to autumn, dropping to 60% in the winter. This could result from the underestimation of turbulent heat fluxes at the flux tower, which occurred at some sites according to FLUXNET (Baldocchi *et al.* 2001). The remaining terms in the energy balance equation are redistributed into the turbulent fluxes according to the observed Bowen ratio. A set of automatic agro-meteorological equipment was also installed to measure routine climate data, including air temperature, relative humidity and wind speed. A groundwater network was used to record the groundwater level and two soil moisture profiles were measured at depths of 5, 10, 20, 40, 80 and 160 cm. The crop growth parameters including LAI, root mass and crop height were sampled every two weeks.

2.2 *Estimating actual ET using P-M model and MODIS data*

The P-M model is based on the energy balance and aerodynamics theory (Monteith 1964):

$$\lambda E = \frac{\Delta(R_n - G_0) + \rho C_p(e^*(T_a) - e_a)/r_a}{\Delta + \gamma(1 + r_s/r_a)}, \tag{1}$$

where E is the mass water ET rate, λ is the latent heat of vaporization, λE together represents the latent heat fluxes (W m^{-2}), R_n is net radiation (W m^{-2}), G_0 is soil heat flux (W m^{-2}), T_a is the air temperature (°C) at reference height, $e^*(T_a)$ and e_a are the saturation vapour pressure (kPa) at temperature T_a and the actual vapour pressure (kPa) respectively. Δ is the slope of the saturated vapour pressure at the air temperature (kPa °C^{-1}), ρ is the air density (kg m^{-3}), C_p is the air specific heat (J kg^{-1} °C^{-1}), γ is the psychrometric constant (kPa °C^{-1}) and r_a is the aerodynamic resistance (S m^{-1}) and r_s is the surface resistance (S m^{-1}), which was mainly influenced by water availability and canopy photosynthesis process. Estimating the surface resistance under water stress was the major difficulty when applying the P-M method on actual ET estimation. Cleugh *et al.* (2007) and Mu *et al.* (2007) used the LAI derived from MODIS data to estimate the surface resistance. However, LAI, similar to Normalized Difference Vegetation Index (NDVI), is more sensitive to the canopy biophysical parameters and may not be able to effectively characterize the surface resistance under water stress conditions.

The radiative transfer model showed that leaf water was the dominant factor influencing the leaf reflectance in the shortwave infrared (SWIR) wavelengths (Ceccato *et al.* 2002). The Normalized Difference Water Index (NDWI) is a combination of the near-infrared (NIR) and SWIR wavelengths, defined as:

$$\mathrm{NDWI} = \frac{\rho_{\mathrm{NIR}} - \rho_{\mathrm{SWIR}}}{\rho_{\mathrm{NIR}} + \rho_{\mathrm{SWIR}}}, \tag{2}$$

where ρ_{SWIR} and ρ_{NIR} are the reflectance in SWIR and NIR wavelengths respectively. NDWI was shown to be sensitive to the canopy water stress and also showed a response to the crop growth at the same time (Fensholt and Sandholt 2003, Jackson

et al. 2004, Chen *et al*. 2005). Moreover, NDWI was more resistant to cloud effect and other atmospheric disturbances (Yi *et al*. 2008). Therefore, the following is more suitable for surface resistance estimation:

$$r_s = r_{s\_max} f(\mathrm{NDWI}) = r_{s\_max}(1 - a(\mathrm{NDWI})), \tag{3}$$

where r_s is the surface resistance (S m^{-1}), and r_{s_max} is the maximum resistance (S m^{-1}) and can be regarded as the resistance when there is no vegetation cover and the soil moisture is close to the wilting point or under water stress. $f(\mathrm{NDWI})$ is a linear expression of NDWI (with a as an empirical coefficient subject to calibration), which describes the influence of surface moisture condition and crop growth. For the crop at the same growth period, NDWI would decrease and surface resistance would increase if the crop suffered water stress. Here the MODIS bands 7 and 2 centred at 2130 nm (SWIR) and 858 nm (NIR) were used to calculate the NDWI index.

A one-layer model was also applied in this area to compare with the P-M model. The heat transfer process between the land surface and atmosphere can be expressed as:

$$H = \rho C_p \frac{T_s - T_a}{r_a + r_{ex}}, \tag{4}$$

where T_s is the radiometric surface temperature (K) and T_a was the air temperature at reference height (K). The excess resistance r_{ex} or a dimensionless heat transfer coefficient B^{-1} (B-sublayer stanton number) was used to adjust the difference between the aerodynamic temperature and surface temperature derived from remote sensing (Stewart *et al*. 1994). B^{-1} is greatly affected by surface vegetation, topography and meteorological condition (Lhomme *et al*. 1997). Here the parameterization scheme proposed in Su *et al*. (2001) integrating the influences of these factors was used to estimate B^{-1}:

$$kB^{-1} = \frac{kC_d}{4C_t \frac{u_*}{u(h)}(1 - e^{-n_{ec}/2})} f_c^2 + \frac{k \frac{u_*}{u(h)} \frac{z_{0m}}{h}}{C_t^*} f_c^2 f_s^2 + kB_s^{-1} f_s^2, \tag{5}$$

where k is the von-Karman constant, f_c and f_s are the coverage fraction of vegetation and soil, respectively, C_d is the leaf dragging coefficient, C_t is the leaf heat transfer coefficient and C_t* is the soil heat transfer coefficient. u_* is the friction velocity (m s^{-1}) and z_{0m} is the roughness height for momentum transfer (m), $u(h)$ is the wind speed at height, h, of the canopy (m s^{-1}), n_{ec} is the within-canopy wind speed profile extinction coefficient, and B_s^{-1} is the dimensionless heat transfer coefficient for bare soil.

2.3 *Flow diagram of the ET models and data sources*

Figure 2 shows flow diagrams of the model processing. Two datasets were required as inputs to the two models. The first dataset consisted of land surface albedo, vegetation indices (including NDWI and NDVI), LAI and surface temperature. These inputs were derived from either daily or composite MODIS land products. The second climate dataset included atmospheric pressure, air temperature, humidity, wind speed, downward solar radiation or daily sunshine hour, which were interpolated from the observations at weather stations.

The surface albedo and downward solar radiation (or daily sunshine hours) were used to calculate the instantaneous (or daily) net shortwave radiation. The instantaneous net longwave radiation was estimated from the surface temperature and air temperature, while only the maximum and minimum air temperatures were required to estimate the daily net longwave radiation. The fractional coverage was used to

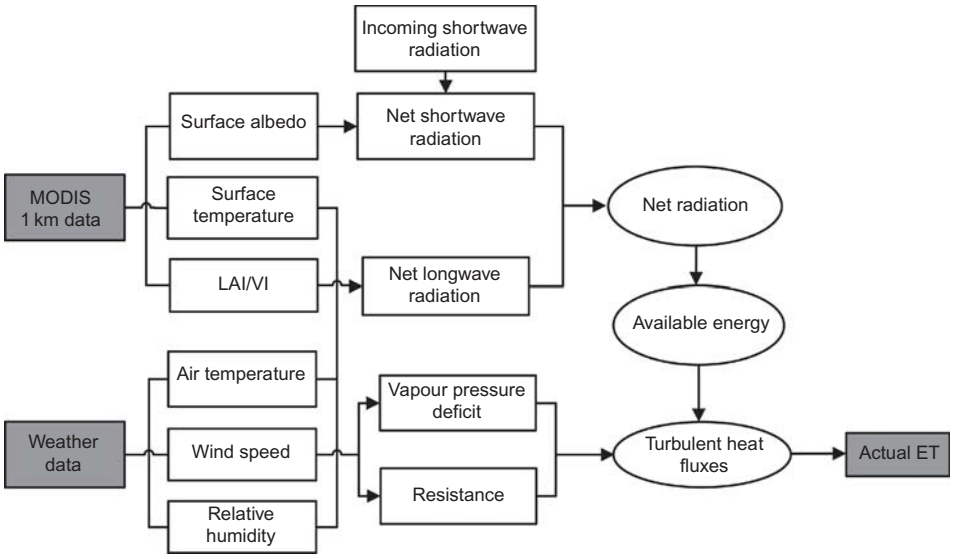

Figure 2. Flow diagram of the evapotranspiration models including the inputs, data processing and the outputs. VI stands for vegetation index.

estimate the soil heat together with the net radiation. The NDVI and LAI provided estimates of vegetation parameters influencing the surface heat transfer process, and a bunch of meteorological variables was used to determine the aerodynamic resistance for the turbulent heat fluxes. NDWI was used to estimate the surface resistance required by the P-M model.

MODIS daily and composite images including surface temperature, surface reflectance, vegetation index (VI) and LAI from 2006 to 2007 were reprojected from the sinusoidal (SIN) projection into the Universal Transverse Mercator (UTM) projection and resampled into 1 km resolution. Images with extensive cloud cover were removed according to the quality flags in the MODIS datasets.

The meteorological data from 2006 to 2007 were also collected at three weather stations as well as the field site (see figure 1). The inverse distance weighting method was used to map the spatial distribution of the meteorological variables. The three stations provided hourly observations in 2006, but only daily observations in 2007. Thus in 2007, the daily data were first interpolated in the whole area and the hourly data were derived, assuming the meteorological variables at all the four sites had similar diurnal curves. This may be reasonable since there was only slight difference in the topography and land cover types across this area. Besides, only the flux tower provided observations of downward shortwave radiation. Therefore, the atmospheric transmissivity was assumed the same across the area and the instantaneous downward shortwave radiation varied solely with the geophysical parameters.

3. Vegetation parameterization using MODIS data

Surface albedo and LAI greatly influenced the energy balance at the surface. The uncertainties in the MODIS albedo and LAI products were analysed and the method to reduce the uncertainties in the input parameters for the ET models was discussed. The MCD43B3 product provided temporal composite surface albedo at three

wavelengths (0.3–0.7, 0.7–5.0 and 0.3–5.0 μm). This product was generated from the MODIS level 1B surface reflectance data using Ross-Li model, combining Terra and Aqua images to reduce the uncertainty in the input surface reflectance (Strahler *et al.* 1999). In the previous studies the surface albedo has usually been derived from the narrowband surface reflectances, followed Liang (2001). Figure 3 shows a comparison of the composite albedo and the albedo calculated from MODIS bands 1–7 from daily Terra and Aqua images in 2007. It can be observed from the figure that the daily albedo fluctuated widely, and may not disclose the true changes in the surface reflective conditions. This was due to large uncertainties in the input daily reflectances, which were sensitive to the changes in the view and azimuth angles of the sensors, and also cloud and aerosol condition (Yi *et al.* 2008). Thus the daily albedo was interpolated from the 8-day composite data as inputs to the ET models.

LAI has been estimated using a VI such as NDVI in most applications. However, the VI was sensitive to atmospheric disturbances, and became saturated with LAI values larger than 3 (Huete *et al.* 2002). The MOD15A2 product provides 8-day composite LAI data with 1-km resolution. This product uses the 3D radiative transfer model to model the canopy bidirectional reflectance (BRDF) and generates a look-up table (LUT). The LAI is retrieved based on the LUT and the MODIS surface reflectance data. However, the empirical relationship between NDVI and LAI is still used when there is no reliable reflectance data during the composite period due to cloud contamination. Thus, the accuracy of LAI retrievals depends mainly on the input reflectance quality. The MODIS Collection 5 land surface products are improved in atmospheric correction and also in the definition of the radiative transfer model compared with Collection 4 products. The effects of these improvements on LAI retrieval are discussed in the following paragraph.

Figure 4 shows a comparison of the temporal series of LAI from different collections at the field site. LAI values in 2006 and 2005 were extracted from collection 4, and the 2007 data were from collection 5. It can be seen from the figure that LAI values in 2006 and 2005 were much smaller than LAI in 2007 especially during the wheat growth period. The LAI series in 2007 were much closer to the ground truth. Figure 5 shows a comparison of the LAI distribution in the study area at similar growth stages. The LAI time series in 2007 (at date of year (DOY) 121) was 8 days

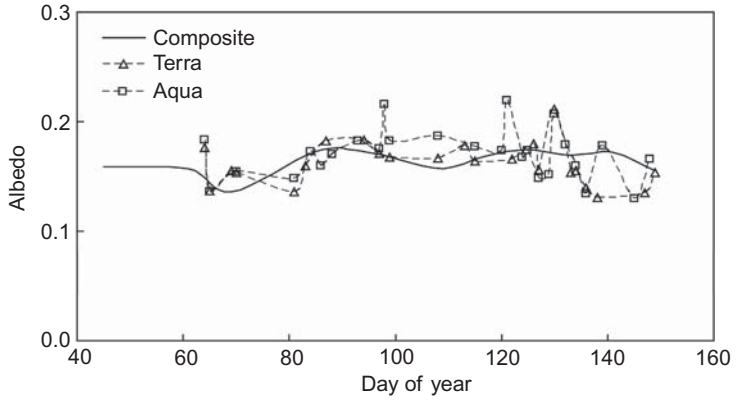

Figure 3. Comparison between the temporal series of surface albedo derived from the MOD43B3 product and the daily surface reflectance in 2007.

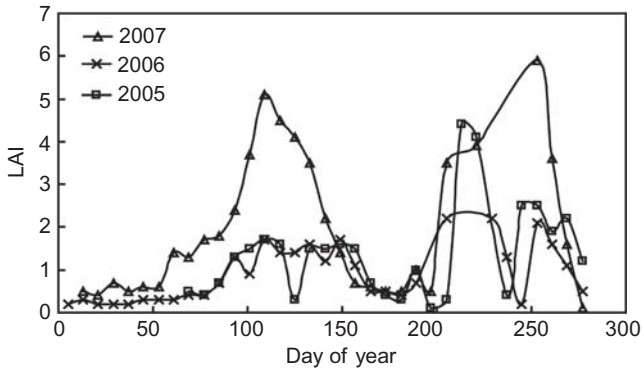

Figure 4. Comparison between the temporal series of LAI extracted from the MODIS products from 2005 to 2007.

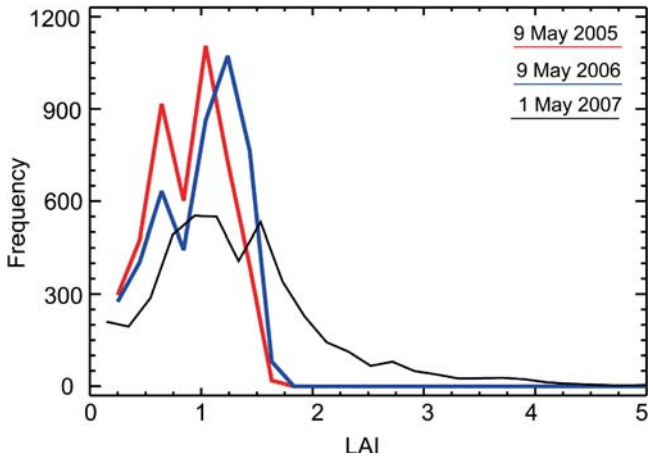

Figure 5. Histogram of LAI distribution in the study area at similar growth periods from 2005 to 2007.

ahead of the LAI series in 2006 and 2005 (at DOY 129) due to the difference in the crop growth cycles. It can be seen that most LAI values in the whole area in 2006 and 2005 were much lower than the values in 2007. However, the wheat was at its growing peak and showed a high LAI at this stage according to the field experiment. From the above analysis, it can be concluded improvements in the LAI retrieval algorithm and also the reflectance quality had contributed greatly to the refinement in the LAI retrievals. Therefore, the LAI values in 2006 were still estimated using the general empirical relationship between the 8-day composite NDVI and LAI. The daily LAI values were then temporally interpolated from the 8-day composite data.

4. Results and discussion

4.1 *P-M model calibration and validation*

Figure 6 shows a comparison of the observed and modelled net radiation and soil heat fluxes in 2007 (*a*) and (*b*) and 2006 (*c*) and (*d*). The P-M model and the one-layer model used the same parameterization for the two flux components, and this

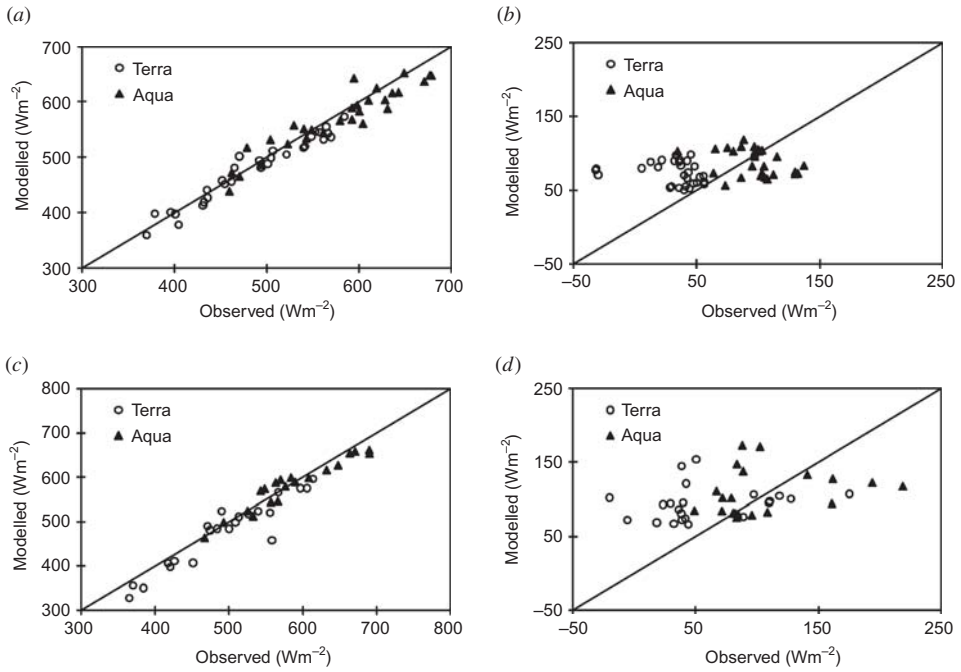

Figure 6. Comparison between the observed and modelled net radiation fluxes in (*a*) 2007 and (*c*) 2006, and soil heat fluxes in (*b*) 2007 and (*d*) 2006, respectively.

parameterization scheme has been widely used in other remote sensing models (Courault *et al.* 2005). In both years, the modelled net radiation results were very close to the observations. In 2007, the root mean square errors (RMSEs) of modelled net radiation were 16.3 and 23.9 W m^{-2} for Terra and Aqua, respectively. In 2006, the RMSE was 30.2 W m^{-2} for Terra and 19.0 W m^{-2} for Aqua, respectively. However, there were large differences between the modelled and observed soil heat fluxes, and the modelled results were generally larger than the observations especially for Terra (in the morning). In 2007, the RMSE of modelled fluxes was as high as 52.1 W m^{-2} for Terra and the RMSE was 33.7 W m^{-2} for Aqua. In 2006, the RMSEs were 60.0 and 47.4 W m^{-2} for Terra and Aqua, respectively. The large discrepancy between the modelled and observed soil heat may be caused by incorrect installation and calibration of the soil heat plates, which should be investigated further.

The flux observations at the overpass time of Aqua from 13:00 to 14:00 hours in 2007 were chosen to calibrate the surface resistance equation (3) and the results are shown in figure 7(*a*). The NDWI and the surface resistance retrieved using the P-M equation showed good linear correlation and the determination coefficient (R^2) was as high as 0.70. The r_{s_max} and a were calibrated as 208.32 S m^{-1} and 1.12, respectively. The calibrated value of surface resistance (r_{s_max}) for bare soil under water stress was in a reasonable range according to the experiment of Daamen and Simmonds (1996) and also the field observations made by Mo *et al.* (2002). The flux observations at the overpass time of Terra at 11:00–12:00 hours in 2007 and both Terra and Aqua in 2006 were used for validation and the modelling results are shown in figure 7(*b*). The modelled latent heat fluxes agreed quite well with the observations. The R^2 values between the modelled and measured latent heat fluxes were 0.94 and 0.84 for 2007

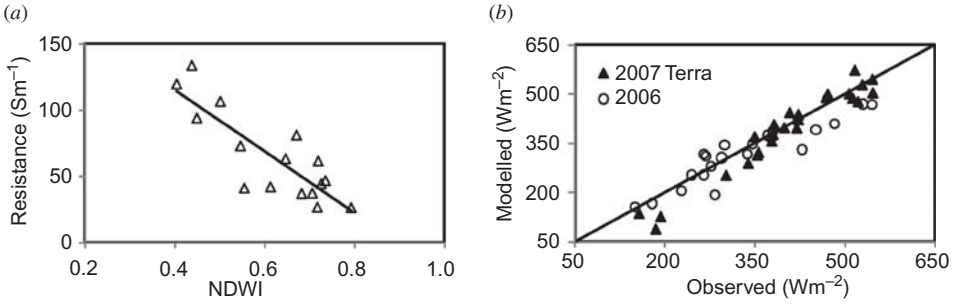

Figure 7. Calibration and validation of surface resistance equation in the P-M model in 2007 and 2006. (*a*) The linear relationship between the surface resistance and NDWI using Aqua data in 2007. (*b*) The modelled latent heat fluxes using calibrated surface resistance for Terra data in 2007 and both Terra and Aqua data in 2006.

Terra and 2006, respectively. The RMSE of the latent heat fluxes was 37.3 W m^{-2} for Aqua in 2007, and 44.7 W m^{-2} in 2006. The RMSE values were comparable with the results from Cleugh *et al.* (2007) but slightly higher than the results from Mu *et al.* (2007). However, the vapour pressure deficit was introduced in Mu *et al.* (2007) to describe the constraint of soil water on the evaporation, which could be reasonable at a large scale. The sensible heat fluxes were derived as the residual of the energy balance equation, so the results were not presented in this article.

Figure 8 shows a comparison of observed and modelled latent heat fluxes by the one-layer model in 2007. The RMSE of the modelled latent heat fluxes was 43.7 W m^{-2} for Terra and 68.8 W m^{-2} for Aqua. The one-layer model showed larger RMSE values than the P-M model, with larger bias under lower latent heat fluxes under smaller vegetation fraction. The one-layer model assumes the land cover is homogeneous and this may be one of the error sources when the land is only partly covered by the crop. The modelling results using Aqua images showed a larger RMSE value than Terra images. However, the relative errors in the morning and afternoon were close because the crop had higher ET in the afternoon. The spatial comparison between the two models was mainly made at the overpass time of Terra in 2007 since the above P-M model was calibrated at the overpass time of Aqua.

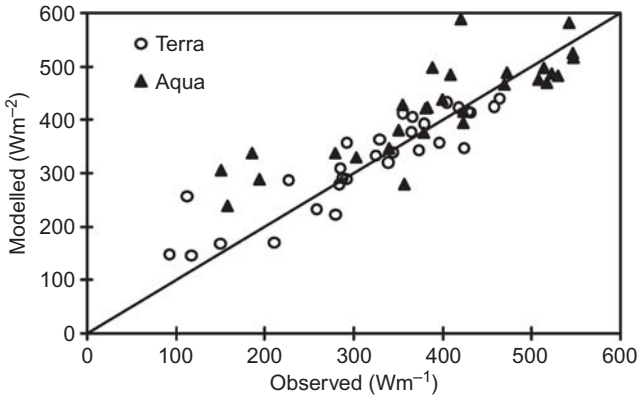

Figure 8. Comparison between the observed and modelled latent heat fluxes by the one-layer model in 2007.

Figure 9 shows comparisons of the spatial distribution of the latent heat fluxes modelled by the two models at three selected dates from April to May in 2007 at the overpass time of Terra. Figure 10 presents histograms of the difference between the modelled latent heat fluxes by the two models at the three dates. The urban and village built-up areas were excluded since the LAI values in these areas were very low and not computed. The areas affected by cloud contamination were also masked as blank areas. It can be seen from figure 9 that the spatial distributions of the fluxes from the two models were quite similar. The latent heat fluxes were generally larger in the irrigated area than the outside of the irrigation zone, and the latent heat fluxes in the north and west areas were much smaller especially in April. These areas were far from the irrigation drainage source at the south east part and usually less irrigated. It can be seen from the figure 9 that typically the one-layer model showed higher ET in wet surfaces and smaller ET in dry surfaces than the P-M model. However, the differences of the modelled latent heat fluxes mainly fell in the range of –50 to +50 W m^{-2}, and were acceptable. However, most of the area in one-layer model showed greater ET than the P-M model on 14 May 2007. The NDWI showed a valley during this period, indicating that the crop may suffer water stress during this period, while the one-layer model showed most of the area had high ET. However, the daily NDWI values were affected by the atmospheric condition and the view angles, which may contribute to this discrepancy.

The above analysis shows the MODIS NDWI can provide reasonable estimation of surface resistance under different soil moisture status and crop growth situations. This was because the NDWI contains information from the SWIR and NIR wavelengths, which are sensitive to the crop water content, and also the accumulation of the dry matter with crop growing (Yi *et al*. 2007).

4.2 *The daily ET time series modelled by the P-M model*

The P-M method was used to estimate the daily water consumption during the wheat growing period in 2006 and 2007. The 8-day temporal composite NDWI was interpolated to daily data and used to estimate the daily surface resistance instead of using the daily MODIS data. Good quality daily MODIS data may not be available due to cloud or other factors, which was a major drawback to the one-layer model. Moreover, the composite process can reduce greatly the uncertainty in the daily surface reflectance caused by the changes in the view and zenith angles, cloud and atmospheric conditions.

Figure 11 shows a comparison between the temporal series of the modelled and observed daily actual ET during the wheat growth period in 2007 and 2006. The eddy covariance observations at heavy rainy days (11 and 30 May 2007 and 25–27 May 2006) were excluded. It can be seen from the figure that the modelled and observed ET time series showed similar trends during the period. The daily ET values showed obvious temporal changes with the crop growth. In 2007, the modelled average daily ET values increased from 2.10 mm day^{-1} in March to 4.32 mm day^{-1} in April and 4.84 mm day^{-1} in May. In 2006, the changes in the daily ET values were similar to the changes in 2007. In this year, the modelled average daily ET values from March to May were 2.35, 3.75 and 4.55 mm day^{-1} respectively. However, in 2006, the modelled daily ET showed an increase during first March, while there was a decreasing trend in the observed daily ET. The daily NDWI was interpolated from the neighbouring 8-day composite NDWI. The quality of MODIS images was greatly affected by cloud in

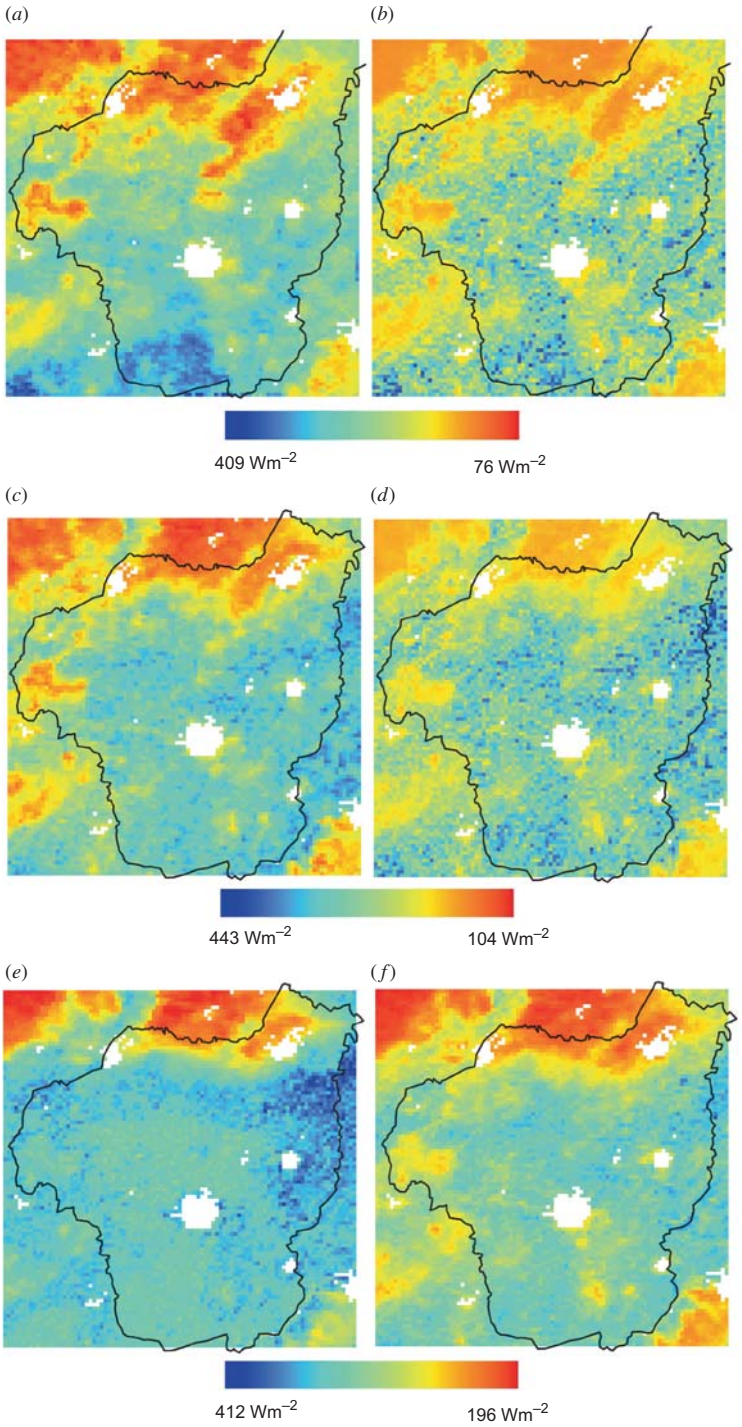

Figure 9. Comparison of the spatial pattern of latent heat fluxes modelled from Terra images of (*a*) 7 April 2007 by the one-layer model; (*b*) 7 April 2007 by the P-M model; (*c*) 25 April 2007 by the one-layer model; (*d*) 25 April 2007 by the P-M model; (*e*) 14 May 2007 by the one-layer model; (*f*) 14 May 2007 by the P-M model. The irrigation area boundary is marked using the black line.

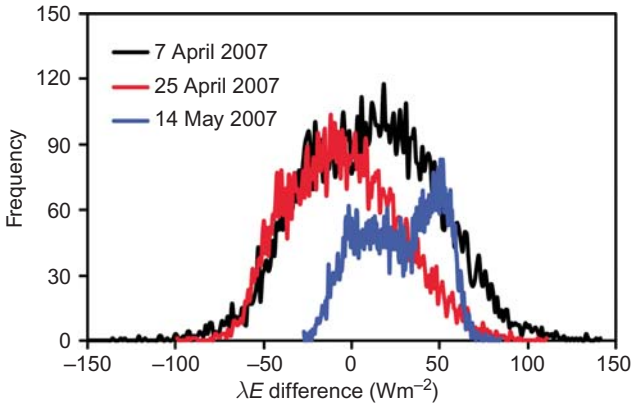

Figure 10. Histograms of the difference between the latent heat fluxes modelled by the P-M model and the one-layer model at the selected dates in 2007.

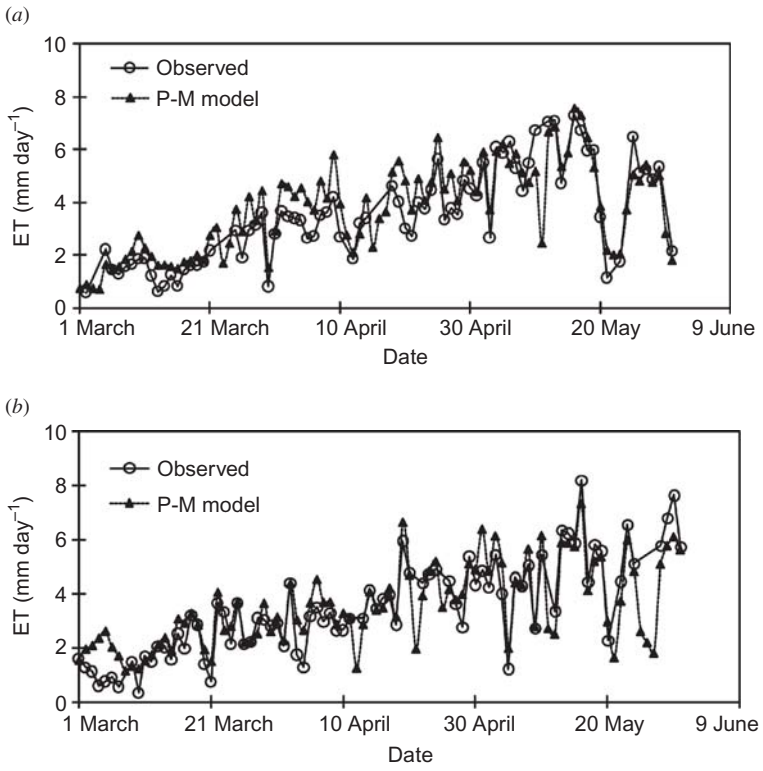

Figure 11. Comparison between the temporal series of the observed and modelled daily evapotranspiration using the P-M model during the wheat season in (*a*) 2007 and (*b*) 2006.

the winter and early spring in this area, and the influence of cloud cannot be totally eliminated even after temporal composite. On the other hand, the 8-day composite NDWI can capture the canopy water stress during a longer period than 8 days, but may not respond to a short-term stress.

The temporal series of observed soil moisture, precipitation and irrigation during the same periods are shown in figure 12. The statistics of the water balance components in the two years are shown in table 1. The total crop water consumption from March to May was estimated to be 344.9 mm in 2007 and 326.5 mm in 2006, while the rainfall amount was lower than 100 mm in both years. The irrigation amount was estimated to be around 150 mm in 2007 and 80 mm in 2006 according to the temporal changes of measured soil moisture profile and groundwater level. Due to water balance, the crop had to extract a large amount of water from the deep soil layer and groundwater to sustain its growth in both years, which were around 194 mm in 2006 and 117 mm in 2007. According to the measured soil moisture and groundwater level, the changes in the total soil water storage in 2006 and 2007 were estimated to be 169.2 and 89.8 mm respectively. The water imbalance amount in 2006 was around 25 and 27 mm in 2007. The estimates of water extraction may be not very accurate because it was difficult to separate the discharge and recharge periods of the groundwater. Also, the horizontal water movement was ignored

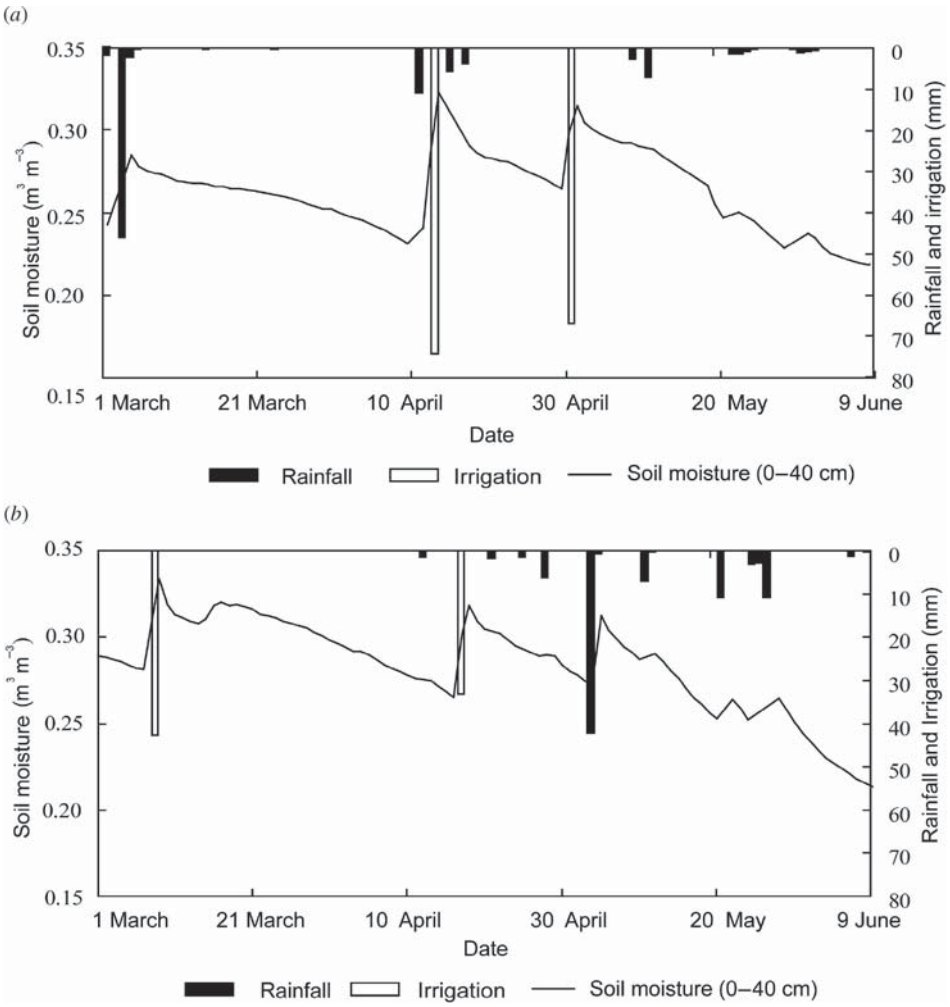

Figure 12. Temporal series of the observed soil moisture, precipitation and irrigation in (*a*) 2007 and (*b*) 2006.

Table 1. The statistics of the water balance components (mm) during the major wheat growing period from March to May in 2006 and 2007.

	ET (model)	Precipitation	Irrigation	ΔSW	Imbalance
2006	363	89	80	169.2	24.8
2007	353	86	150	89.8	27.2

Note: ΔSW is the amount of water extracted by the crop from the deep soil layer and groundwater, calculated from the measured soil moisture profiles and groundwater level.

during the calculation. Compared with 2007, the wheat consumed more water from the root zone and deep soil layer in 2006 due to less irrigation, which was indicated by the sharp decrease in the soil moisture and increase in the groundwater level. It can be also seen from figure 12 that the initial soil moisture in 2006 was slightly higher than in 2007, and correspondingly the actual ET in March 2006 was slightly larger than in 2007. However, the rainfall and irrigation amounts were lower in 2006 than in 2007, and therefore 2007 had larger ET during the later period.

5. Conclusions

An operational method using MODIS data was proposed to estimate the crop water consumption, and was applied in an irrigated wheat area along the downstream part of the Yellow River. MODIS NDWI was used to characterize the surface resistance and the P-M model was used to model the daily actual ET during the wheat growing season from March to April.

The ET models were quite sensitive to the input vegetation parameters, especially albedo and LAI. It was found that the temporal composite MODIS products provided more reasonable estimates of these two parameters than the daily products. Thus a vegetation parameterization retrieval scheme using the temporal-composite MODIS data was employed.

NDWI was shown to provide reasonable estimation of surface resistance for P-M model at different crop growth condition and soil moisture status. The latent heat fluxes modelled by P-M agreed well with the field observations and showed similar spatial pattern to those from the one-layer model. To avoid the discontinuousness in the availability of the remote sensing images due to cloud effects, 8-day temporal composite MODIS data were used to generate the daily NDWI and surface resistance and the P-M model was used to estimate the daily actual ET. Compared with the observed precipitation, irrigation and soil moisture curves, the modelled daily ET curves provided reasonable estimation of crop consumption during the wheat major growing period. Moreover, this model showed obvious advantages over the other remote sensing models, which require inputs of radiometric temperature, since the availability of these data was greatly influenced by the weather conditions and subjected to great uncertainty. Therefore, this model can provide continuous estimation of daily crop water consumption at a regional scale and showed great potential in precision irrigation management.

Acknowledgements

This research was supported by the National 973 Project of China (2006CB403405) and the National Natural Science Founding Projects of China (50679029).

References

Baldocchi, D., Falge, E., Gu, L., Olson, R., Hollinger, D., Running, S., Anthoni, P., Bernhofer, C., Davis, K., Evans, R., Fuentes, J., Goldstein, A., Katul, G., Law, B., Lee, X., Malhi, Y., Meyers, T., Munger, W., Oechel, W., Paw, U.K., Pilegaard, K., Schmid, H., Valentini, R., Verma, S., Vesala, T., Wilson, K. and Wofsy, S., 2001, FLUXNET: a new tool to study the temporal and spatial variability of ecosystem-scale carbon dioxide, water vapor, and energy flux densities. *Bulletin of American Meteorological Society*, **82**, pp. 2415–2434.

Bastiaanssen, W.G.M., Menenti, M., Feddes R.A. and Holtslag, A.A.M., 1998, A remote sensing surface energy balance algorithm for land (SEBAL) (1. Formulation). *Journal of Hydrology*, **212–213**, pp. 198–212.

Ceccato, P., Gobron, N., Flasse, S., Pinty, B. and Tarantola, S., 2002, Designing a spectral index to estimate vegetation water content from remote sensing data: Part 1. Theoretical approach. *Remote Sensing of Environment*, **82**, pp. 188–197.

Chehbouni, A., Lo Seen, D., Njoku, E.G. and Monteny, B., 1996, Examination of the difference between radiative and aerodynamic surface temperatures over sparsely vegetated surface. *Remote Sensing of Environment*, **58**, pp. 177–186.

Chehbouni, A., Nouvellon, Y., Lhomme, J., Watts, C., Boulet, G., Kerr, H., Moran, S. and Goodrich, D., 2001, Estimation of surface sensible heat flux using dual angle observations of radiative surface temperature. *Agricultural and Forest Meteorology*, **108**, pp. 55–65.

Chen, D., Huang, J. and Jackson, T.J., 2005, Vegetation water content estimation for corn and soybeans using spectral indices derived from MODIS near- and short-wave infrared bands. *Remote Sensing of Environment*, **98**, pp. 225–236.

Cleugh, H.A., Leuning, R., Mu, Q. and Running, S.W., 2007, Regional evaporation estimates from flux tower and MODIS satellite data. *Remote Sensing of Environment*, **106**, pp. 285–304.

Courault, D., Seguin, B. and Olioso, A., 2005, Review on estimation of evapotranspiration from remote sensing data: from empirical to numerical modeling approaches. *Irrigation and Drainage Systems*, **19**, pp. 223–249.

Cracknell, A.P. and Varotsos C.A., 2007, The IPCC fourth assessment report and the fiftieth anniversary of Sputnik. *Environmental Science and Pollution Research*, **14**, pp. 384–387.

Daamen, C.C. and Simmonds, L.P., 1996, Measurement of evaporation from bare soil and its estimation using surface resistance, *Water Resources Research*, **32**, pp. 1393–1402.

Fensholt, R. and Sandholt, I., 2003, Derivation of a shortwave infrared water stress index from MODIS near- and shortwave infrared data in a semiarid environment. *Remote Sensing of Environment*, **87**, pp. 111–121.

French, A.N., Jacob, F., Anderson, M.C., Kustas, W.P., Timmermans, W., Gieske, A., Su, Z., Su, H., McCabe, M.F., Li, F., Prueger, J. and Brunsell, N., 2005, Surface energy fluxes with the Advanced Spaceborne Thermal Emission and Reflection radiometer (ASTER) at the Iowa 2002 SMACEX site (USA). *Remote Sensing of Environment*, **99**, pp. 55–65.

Huete, A., Didan, K., Miura, T., Rodriguez, E.P., Gao, X. and Ferreira, L.G., 2002, Overview of the radiometric and biophysical performance of the MODIS vegetation indices. *Remote Sensing of Environment*, **83**, pp. 195–213.

Jackson, T.J., Chen, D., Cosh, M., Li, F., Anderson, M., Walthall, C., Doriaswamy, P. and Hunt, E.R., 2004, Vegetation water content mapping using Landsat data derived normalized difference water index for corn and soybeans. *Remote Sensing of Environment*, **92**, pp. 475–482.

Jiang, L. and Islam, S., 1999, A methodology for estimation of surface evapotranspiration over large areas using remote sensing observations. *Geophysical Research Letters*, **26**, pp. 2773–2776.

Jupp, D.L.B., Tian, G., McVicar, T.R., Qin, Y. and Li, F., 1998, *Soil Moisture and Drought Monitoring using Remote Sensing I: Theoretical Background and Methods*. CSIRO Earth Observation Centre Report 98/1 (CSIRO: Canberra).

KATUL, G.G., SCHIELDGE, J., HSIEH, C.I. and VIDAKOVIC, B., 1998, Skin temperature perturbations induced by surface layer turbulence above a grass surface. *Water Resources Research*, **34**, pp. 1265–1274.

KUSTAS, W.P. and NORMAN J.M., 1999, Evaluation of soil and vegetation heat flux predictions using a simple two-source with radiometric temperatures for partial canopy cover. *Agricultural and Forest Meteorology*, **94**, pp. 13–29.

KUSTAS, W.P., NORMAN, J.M., ANDERSON, M.C. and FRENCH, A.N., 2003, Estimating subpixel surface temperatures and energy fluxes from the vegetation index-radiometric temperature relationship. *Remote Sensing of Environment*, **85**, pp. 429–440.

LHOMME, J.P., MONTENY B., TROUFLEAU, D., CHEHBOUNI, A. and BAUDUIN S., 1997, Sensible heat flux and radiometric surface temperature over sparse Sahelian vegetation II. A model for the kB-1 parameter. *Journal of Hydrology*, **188–189**, pp. 839–854.

LIANG, S., 2001, Narrowband to broadband conversions of land surface albedo I algorithms. *Remote Sensing of Environment*, **76**, pp. 213–238.

MAAYAR, M. and CHEN J., 2006, Spatial scaling of evapotranspiration as affected by heterogeneities in vegetation, topography, and soil texture. *Remote Sensing of Environment*, **102**, pp. 33–51.

MO, X., LIU, S. and LIN, Z., 2002, Energy balance, water use efficiency and surface resistance in a maize field. *Chinese Journal of Applied Ecology*, **13**, pp. 551–554.

MONTEITH, J.L., 1964, Evaporation and environment. The state and movement of water in living organisms. In *Symposium of the Society of Experimental Biology*, **19**, pp. 205–234. (Cambridge: Cambridge University Press).

MORAN, M.S., CLARKE, T.R., INOUE, Y. and VIDAL, A., 1994, Estimating crop water deficit using the relation between surface air temperature and spectral vegetation index. *Remote Sensing of Environment*, **49**, pp. 246–263.

MU, Q., HEINSCH, F., ZHAO, M. and RUNNING, S., 2007, Development of a global evapotranspiration algorithm based on MODIS and global meteorology data. *Remote Sensing of Environment*, **111**, pp. 519–536.

NISHIDA, K., NEMANI, R.R., RUNNING, S.W. and GLASSY, J.M., 2003, An operational remote sensing algorithm of land surface evaporation. *Journal of Geophysical Research*, **108**, pp. 4270–4283.

NORMAN, J.M., KUSTAS, W.P. and HUMES, K.S., 1995, A two-source approach for estimating soil and vegetation energy fluxes in observations of directional radiometric surface temperature. *Agricultural and Forest Meteorology*, **77**, pp. 263–293.

STEWART, J.B., KUSTAS, W.P., HUMES, K.S., NICHOLS, W.D., MORAN, M.S. and de BRUIN, H.A.R., 1994, Sensible heat flux-radiometric surface temperature relationship for eight semiarid areas. *Journal of Applied Meteorology*, **33**, pp. 111–117.

STRAHLER, A.H. and MULLER, J.P., 1999, MODIS BRDF/Albedo product: algorithm theoretical basis document (ATBD) Version 5.0. Available online at: modis.gsfc.nasa.gov/data/atbd/atbd_mod09.pdf.

SU, Z., SCHMUGGE, T., KUSTAS, W.P. and MASSMAN, W.J., 2001, An evaluation of two models for estimation of the roughness height for heat transfer between the land surface and the atmosphere. *Journal of Applied Meteorology*, **40**, pp. 1933–1951.

SU, Z., YACOB, A., WEN, J., ROERINK, G., HE, Y., GAO, B., BOOGAARD, H. and DIEPEN, C., 2003, Assessing relative soil moisture with remote sensing data: theory, experimental validation, and application to drought monitoring over the North China Plain. *Physics and Chemistry of the Earth*, **28**, pp. 89–101.

VAROTSOS, C., 2005, Modern computational techniques for environmental data; Application to the global ozone layer. In *Lecture Notes in Computer Science*, V.S. Sunderam (Ed.), pp. 504–510 (Berlin: Springer).

VAROTSOS, C., ASSIMAKOPOULOS, M.-N. and EFSTATHIOU, M., 2007, Technical Note: Long-term memory effect in the atmospheric CO_2 concentration at Mauna Loa. *Atmospheric Chemistry and Physics*, **7**, pp. 629–634.

Wan, Z., Zhang, Y., Zhang, Q. and Li, Z.L., 2002, Validation of the land surface-temperature products retrieved from Terra Mode rate Resolution Imaging Spectroradiometer data. *Remote Sensing of Environmen*t, **83**, pp. 163–180.

Yang, D., Li, C., Hu, H., Lei, Z., Yang, S., Kusuda, T., Koike, T. and Musiake, K., 2004, Analysis of water resources variability in the Yellow River of China during the last half century using historical data. *Water Resources Research*, **40**, pp. 13–19.

Yi, Y., Yang, D., Chen, D. and Huang J., 2007, Retrieving crop physiological parameters and assessing water deficiency using MODIS data during winter wheat growing period. *Canadian Journal of Remote Sensing*, **33**, pp. 189–202.

Yi, Y., Yang, D., Huang, J. and Chen, D., 2008, Evaluation of MODIS surface reflectance products for wheat leaf area index (LAI) retrieval. *ISPRS Journal of Photogrammetry and Remote Sensing*, **63**, pp. 661–677.